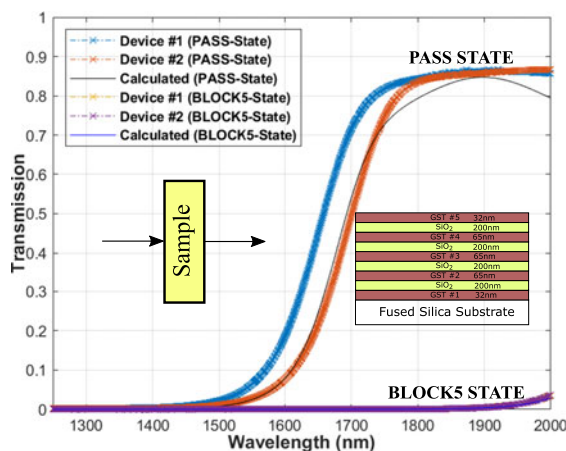


Broadband Reflective Optical Limiter Using GST Phase Change Material

Volume 10, Number 1, February 2018





Andrew Sarangan, *Senior Member, IEEE*
Josh Duran
Vladimir Vasilyev
Nicholaos Limberopoulos, *Member, IEEE*
Ilya Vitebskiy
Igor Anisimov



DOI: 10.1109/JPHOT.2018.2796448

1943-0655 © 2018 IEEE

Broadband Reflective Optical Limiter Using GST Phase Change Material

Andrew Sarangan ¹, Senior Member, IEEE, Josh Duran ²,
Vladimir Vasilyev,² Nikolaos Limberopoulos ², Member, IEEE,
Ilya Vitebskiy ² and Igor Anisimov ²

¹Department of Electro Optics and Photonics, University of Dayton, 300 College Park,
Dayton, OH 45469 USA

²Air Force Research Laboratory, Wright-Patterson AFB, OH 45433 USA

DOI:10.1109/JPHOT.2018.2796448

1943-0655 © 2018 IEEE. Translations and content mining are permitted for academic research only.
Personal use is also permitted, but republication/redistribution requires IEEE permission.
See http://www.ieee.org/publications_standards/publications/rights/index.html for more information.

Manuscript received November 21, 2017; revised January 15, 2017; accepted January 16, 2018. Date of publication January 23, 2018; date of current version March 29, 2018. This work was supported by the AFOSR Summer Faculty Fellowship program. The work of I. Vitebskiy and N. Limberopoulos was supported by AFOSR LRIR 14RY14COR and 16RYCOR335. Corresponding author: Andrew Sarangan (e-mail: sarangan@udayton.edu).

Abstract: We experimentally demonstrate a thermally induced reflective optical limiter using $\text{Ge}_2\text{Sb}_2\text{Te}_5$ (GST) and SiO_2 in a multilayer photonic bandgap edge-filter configuration. In the PASS state, greater than 80% transmission was achieved at $\lambda \sim 1500$ nm over a 300 nm spectral bandwidth and $\pm 45^\circ$ angles of incidence. In the BLOCK state, extinction ratios higher than 30 dB were achieved. By comparison, all previous optical limiters based on nonlinear photonic crystals have severe spectral bandwidth and/or angle of incidence limitations in either the PASS or BLOCK states. A nine-layer implementation of this device was fabricated and tested in this paper. Numerical modeling results show reasonable agreement with measured values. To the best of our knowledge, this is the first demonstration of optical limiting over a broad spectral band using phase change materials with this level of performance. However, it should be noted that although GST can be switched in both directions, the experimental results demonstrated in this paper are limited to PASS-to-BLOCK switching only.

Index Terms: Optical properties of photonic materials, multilayer interference coatings, fabrication and characterization, photonic bandgap structures.

1. Introduction

Optical limiters protect sensitive systems such as cameras, electronics, and the human eye from high-level laser radiation, while allowing normal levels of radiation to pass through. Current generation of optical limiters utilize materials with strong nonlinear absorption [1], [2] or are based on carbon-based suspensions [3]. Common drawbacks of these methods include high limiting thresholds, and low damage thresholds due, mostly, to overheating. One potential solution is to utilize a reflective optical limiter where most of the incident energy is reflected back instead of being absorbed. For example, a resonant microcavity containing a thin film with nonlinear absorption was shown to become highly reflective upon exposure to a high intensity radiation [4]. However, the main limitation of this method, or any other method that relies on resonant transmission, is the narrow transmission bandwidth and angular sensitivity. This limitation may be acceptable in communication and LADAR applications that operate over a narrow spectral range, but most other

applications such as imaging and spectroscopy require transparency over a broad spectral range and incident angles. Hence, a different approach is needed for these applications.

In this paper, we experimentally demonstrate a reflective optical limiter/switch using phase change materials (PCM). These materials experience a physical change in response to an external stimulus, such as temperature. One of the most studied PCM for optical limiting is vanadium dioxide (VO_2), which undergoes a reversible phase change from a semiconducting to a metallic state [5], [6]. However, several aspects of this material have hampered its application in devices, namely high deposition temperatures and a limited number of substrates on which it can be deposited. On the other hand, $\text{Ge}_2\text{Sb}_2\text{Te}_5$ (GST) is a chalcogenide glass that undergoes an amorphous to crystal phase transition [7]. Most importantly, it can be deposited on virtually any substrate or film at low temperatures, and this makes it possible to use it in complex multilayer structures. The transition from amorphous to crystalline phase induces enormous changes in its optical constants in relatively fast time scales on the order of picoseconds to nanoseconds [8]. As a result, a large number of tunable photonic devices have been demonstrated using GST as the active material [9]–[11]. However, unlike VO_2 , this phase change is nonvolatile; i.e., while it will crystallize easily, reverting to its amorphous state requires heating to a higher temperature followed by a fast quench. Although this is routinely done in PCRAM [12] and optical discs [13], it does introduce some additional complexities in the case of an optical limiter.

The device demonstrated in this paper is based on a photonic bandgap edge-filter configuration using GST and SiO_2 as the high and low index films. We show that it is possible to shift the transition edge of the filter by several hundred nanometers by utilizing the huge changes in the refractive index of GST. This shift is orders of magnitude larger than that achievable with nonlinear refraction and, therefore, has the potential to provide a genuinely broadband protection from high-power laser radiation. The heat-induced amorphous-to-crystal transition of GST requires some initial linear optical absorption, which puts some limitation on the low-intensity transmittance. Still, the 84% linear transmittance demonstrated in our device is sufficiently transparent for most applications. For this study, we assume the spectral window of interest to be in the SWIR band between 1500 nm and 2000 nm, but our approach is flexible enough to be adapted to any spectral range in the SWIR or MWIR. In particular, this design has the potential to provide a greatly enhanced protection from high-power laser radiation compared to all other methods, while ensuring a broad spectral band and wide acceptance angle in the PASS and BLOCK states.

Finally, it should be pointed out that in this particular work, the PASS-to-BLOCK transition is achieved by external heating, rather than by exposure to high-intensity laser radiation. This method of heating does not allow us to observe the dynamics of the transition. Nevertheless, the mechanics of heating should not affect the properties of the resulting PASS and BLOCK states. The simpler heating method allows us to evaluate the effectiveness of the designs without complicated optical setups. However, this also limits our ability to reset the device. Therefore, in the current implementation, the device functions only as a single-use limiter, but it is not intrinsically limited to this function.

2. Optical Constants and Phases of GST

Although $\text{Ge}_2\text{Sb}_2\text{Te}_5$ is widely used in electronic memory applications, there are discrepancies in the reported values for its optical constants in the SWIR and MWIR spectra [10], [14], [15]. These are most likely due to differences in deposition techniques and process conditions used in these studies. Before designing a multilayer structure, the optical constants of GST and their repeatability must be determined using the intended deposition process.

$\text{Ge}_2\text{Sb}_2\text{Te}_5$ can be deposited using a number of different physical and chemical vapor deposition methods. In this work, we have focused only on sputter deposition, primarily due to its versatility, low cost and manufacturing scalability. The films in this study were deposited from a 3-inch sputter target, using Ar as the feed gas at 4 mT pressure and 100 W discharge power. The target was initially conditioned for several hours to reach the steady state surface composition required for producing stoichiometrically correct films. Different film thicknesses between 100 nm and 350 nm were made.

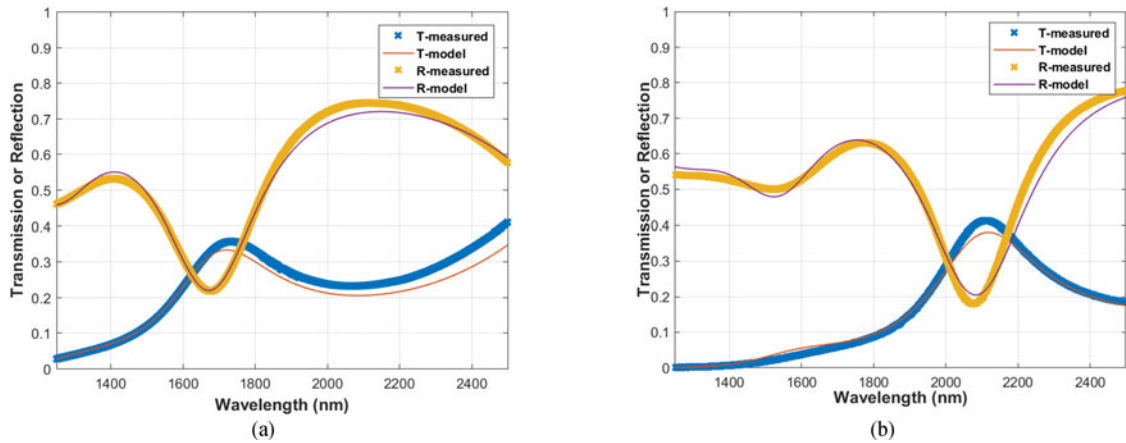


Fig. 1. Reflection & transmission spectra (measured data and best-fit) of 350 nm GST films on fused silica annealed at (a) 145 °C, and (b) 175 °C.

Test coupons were taken from each sample and annealed at different temperatures between 100 °C and 300 °C for 60 seconds. FTIR transmission scans (at normal incidence) and reflection scans (at 10-deg incidence) were taken between 1250 nm and 2500 nm. The transmission was taken at normal incidence, and reflection was taken at 10-deg incidence and was normalized to a gold reflection standard. Fused silica substrates measuring 3 × 1 inch were used for this work, and their optical properties were separately extracted and used in a Transfer Matrix Model to ensure that the substrate properties were self-consistently included in the model. Different dispersion models were used to fit the data, including the Cauchy absorbing, Lorentz and Drude models. For this wavelength range, the best fits were obtained using the Cauchy absorbing dispersion model given by

$$n = A_0 + \frac{10^6 A_1}{\lambda^2} + \frac{10^{12} A_2}{\lambda^4} + \frac{10^{18} A_3}{\lambda^6} \quad (1)$$

$$\kappa = B_0 + \frac{10^6 B_1}{\lambda^2} + \frac{10^{12} B_2}{\lambda^4} \quad (2)$$

where λ is in nanometers. A numerical minimization routine was utilized to simultaneously optimize for the film's complex refractive index $n - j\kappa$ and thickness t in the 1250 nm–2500 nm spectral range. The average error between the measured and calculated spectra was then used to compute the “goodness of fit” (GOF) parameter. The GOF for all temperature values were greater than 95%, with the majority of them close to 99%. For example, Fig. 1(a) and (b) show the measured reflection and transmission spectra from a 350 nm GST film on fused silica for two anneal temperature values of 145 °C and 175 °C, along with their corresponding analytical fits.

Fig 2(a) and (b) show the extracted n and κ values for all anneal temperatures. The as-deposited (un-annealed) samples are indicated by “AD”. We can identify two groupings in the dispersion curves. The amorphous state has refractive index values in the range of 3.75–4.5. When annealed above 145 °C the values jump to 5.0–6.5 due to the phase transition from amorphous to a cubic crystalline phase. Above 200 °C, the film switches to a hexagonal crystalline phase, and the measured spectra contain fewer distinct features to reliably extract their n and κ values. A 10% reduction in film thickness is also observed when the film is annealed above 145 °C, which can be attributed to the densification due to crystallization [16].

To verify the phase transition of the films, X-ray diffraction analysis was performed using an X-ray diffractometer with a hybrid monochromator and Cu $K\alpha_1$ radiation ($\lambda = 1.5406 \text{ \AA}$). Symmetrical $\omega - 2\theta$ scan method was used to define out-of-plane diffraction peaks. Fig. 3 shows the XRD patterns that characterize the as-deposited amorphous film and its transformation to the crystalline phases after annealing at 175 °C, 200 °C, and 300 °C. The film annealed at 175 °C is crystallized into a face-centered cubic phase shown by the XRD peaks [111], [002], [022], [222], and [024],

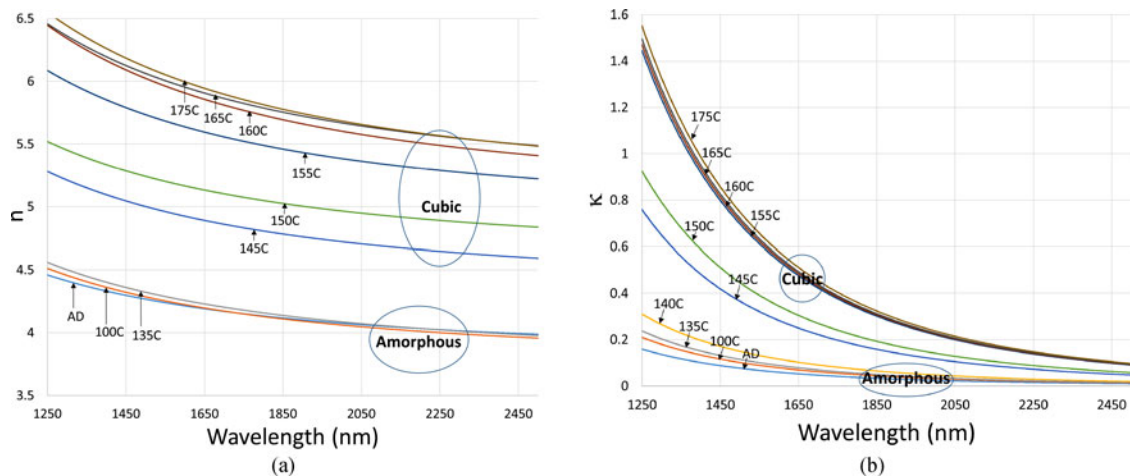


Fig. 2. Experimentally determined refractive index values for (a) n ; and (b) κ as a function of wavelength for all anneal temperatures.

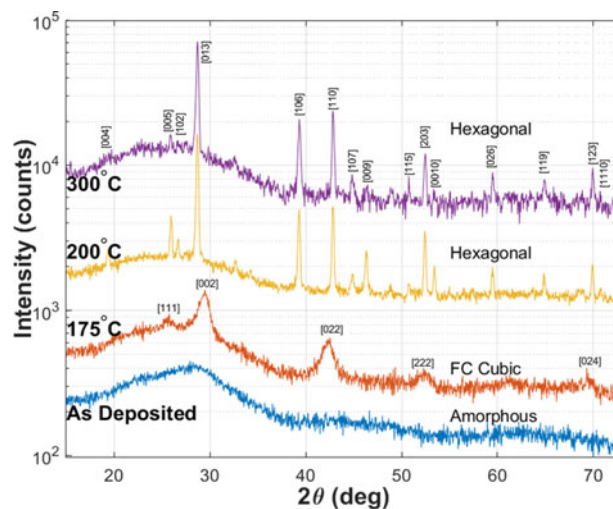


Fig. 3. XRD plot of as-deposited (amorphous) and annealed GST films at 175 °C, 200 °C, and 300 °C.

which are typical for the NaCl like cubic cell [17], [18]. The formation of cubic crystalline phase starts at 150 °C, and exists up to 175 °C. Further annealing at temperatures above 175 °C leads to the restructuring of the cubic cell and the appearance of new XRD peaks that belong to the hexagonal phase with the most likely stoichiometry of $\text{Ge}_2\text{Sb}_2\text{Te}_5$ [17]. The cubic-hexagonal transformation starts at temperatures in the range of 175 °C–200 °C and fully completes at 250 °C. No presence of cubic phase XRD peaks was revealed at temperatures above 200 °C.

3. Multilayer Design & Analysis

The layer structure shown in Fig. 4 was designed as a photonic bandgap long-pass edge filter consisting of four unit cells of $(\frac{G}{2}L\frac{G}{2})$ where G is a quarter-wave thick GST film, and L is a quarter-wave thick SiO_2 film at a reference wavelength λ_0 . A short-pass configuration can also be used, with a unit cell of $(\frac{L}{2}G\frac{L}{2})$, but would require thicker films because the reference wavelength λ_0 will be longer. Details of the design methodologies can be found elsewhere [19]. Given the large index contrast between GST and SiO_2 , only a few repeating unit cells are required to achieve a large

GST #5	32nm
SiO ₂	200nm
GST #4	65nm
SiO ₂	200nm
GST #3	65nm
SiO ₂	200nm
GST #2	65nm
SiO ₂	200nm
GST #1	32nm
Fused Silica Substrate	

Fig. 4. Layer structure of the $(\frac{G}{2} L \frac{G}{2})^4$ device.

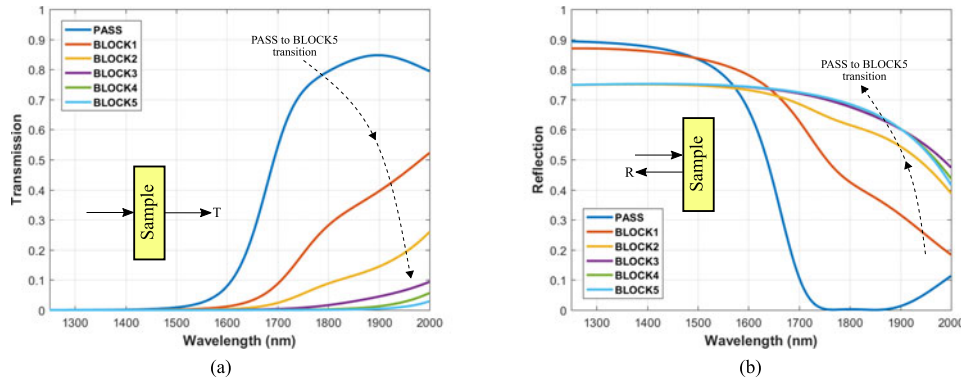


Fig. 5. Simulated transmission and reflection as a function of wavelength for the different switching states.

difference between the transmitted and reflected portions of the long-pass filter. In this case we consider four repeating unit cells such as $(\frac{G}{2} L \frac{G}{2})^4$. The device is designed to be in the PASS-state when all GST layers are in their amorphous states. The BLOCK state occurs in several incremental steps, as each GST layer switches to the cubic crystalline state. Because there are five GST layers, we will designate these states as BLOCK1, BLOCK2,... BLOCK5.

Using $\lambda_0 = 1155 \text{ nm}$, $n_G \approx 4.4$ and $n_L \approx 1.45$, the quarter-wave film thicknesses will be $t_G = \frac{1155}{4 \times 4.4} \approx 65 \text{ nm}$ and $t_L = \frac{1155}{4 \times 1.45} \approx 200 \text{ nm}$ for the GST and SiO₂ films, respectively. Since the optical dispersion of GST is quite strong, analytical expressions for the stop-band and pass-band characteristics are not very useful in this case. Instead, the film structure along with the measured dispersion curves shown in Fig. 2 were used in a numerical transfer matrix model (TMM) to predict the performance of the multilayer structure at the different switching states.

As shown in Fig. 5(a) and (b) in the PASS state (when all GST films are in the amorphous state) the maximum transmission in the passband is 84.7%, and the maximum reflection in the stop band is 89.3%. In the BLOCK5 state (when all GST films have switched to the cubic crystalline phase), the transmission drops to nearly zero at all wavelengths within the 1250 nm–2000 nm band, and the reflection and absorption remains relatively flat with an average value of approximately 75% and 25% respectively. Considering illumination with a 1680 nm laser, GST #4 will incur the highest absorption of 12.4%. Therefore, neglecting any thermal crosstalk between the layers, GST #4 will switch first to the cubic crystalline phase to bring the system to BLOCK1. In the BLOCK1-state, GST #5 will have the second highest absorption of 7.6%, and will switch next. Following the same line of argument, the switching sequence can be shown to be GST #4 → GST #5 → GST #3 → GST #2 → GST #1. In other words, switching will take place sequentially layer by layer due to the redistribution of the optical field in the structure as each GST layer changes its phase.

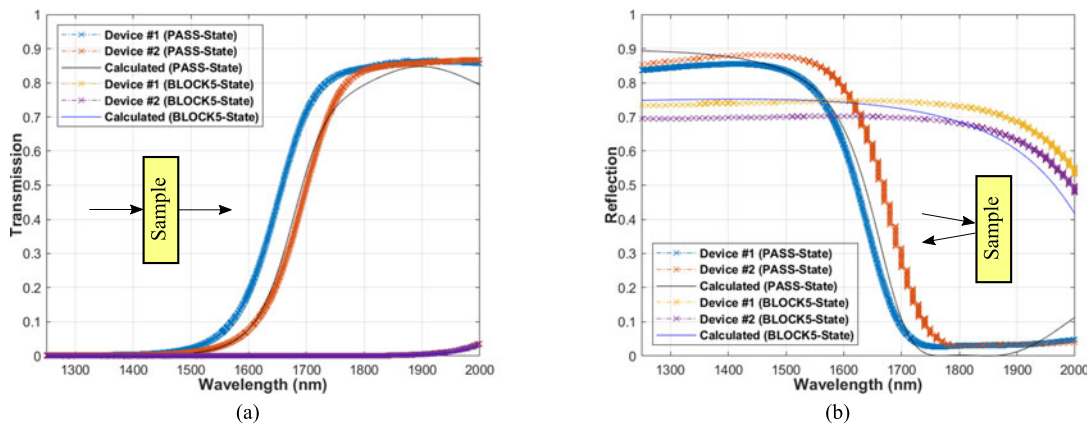


Fig. 6. Measured transmission (at normal incidence) and reflection (at 10-deg incidence) compared to the calculated results for the PASS and BLOCK5 states.

4. Experimental Results

The structure as shown in Fig. 4 was fabricated using Ar^+ RF sputter deposition of $\text{Ge}_2\text{Sb}_2\text{Te}_5$ and SiO_2 layers on silica glass substrates. The layer structure was $(\frac{G}{2}L\frac{G}{2})^4$ where G is a quarter-wave thick (65 nm) GST film and L is a quarter-wave thick (200 nm) SiO_2 film, resulting in a total of 9 layers. The deposition was carried out one layer at a time using rate and time to control the film thickness, and verifying the thickness on a companion sample after each layer using a profilometer. The profilometer used for this work had a vertical resolution of 1.5 \AA with a repeatability of 0.1%. After all layers were deposited, the sample was separated into smaller pieces for annealing at different temperatures. Spectral measurements were taken from two samples (Device #1 and Device #2) that were adjacent on the substrate plate to evaluate the uniformity and consistency of the results. The two devices were approximately three inches apart on the substrate holder, and therefore, represent typical deviations one could expect in performance due to film thickness nonuniformities, which were calibrated to be within $\pm 2\%$.

Transmission and reflection measurements were performed using FTIR spectroscopy between the wavelengths of 1250 nm and 2000 nm. Transmission was taken at normal incidence and reflection was taken at a 10° incidence. Fig. 6(a) and (b) show the measured scans when the GST layers are in their as-deposited amorphous state (PASS state), and also when GST layers are in the cubic crystalline state at 175°C (BLOCK5 state). In the PASS state the transmission turns on at around 1550 nm, reaches a peak value of 85% at 1896 nm, and continues to remain above 80% up to 2000 nm. In the BLOCK5 state, the transmission falls to nearly zero across the entire spectral band. Similarly, reflection remains below 10% for all wavelengths above 1700 nm in the PASS state, and rises above 60% in the BLOCK5 state. The plots show the measured values from two different devices as well as the calculated values using the transfer matrix model (which are the same PASS and BLOCK5 states shown in Fig. 5(a) and (b)). We observe that the agreement between the measurement and simulation is generally very consistent, and most of the deviations are at the longer wavelengths where the refractive index data for GST was less reliable.

Fig. 7 shows the measured extinction ratio compared with model predictions. The extinction is defined as the ratio of the transmission values between the PASS and BLOCK5 states. The slightly lower measured ratios compared to the model and the scatter in the data can be attributed to the noise floor in the measurement system, especially at the shorter wavelength range where the transmission values in both states are so small that thermal noise becomes a major contributing factor in the measured data. Nevertheless, the agreement with the model can be considered reasonably close given the fabrication tolerances, measurement accuracies, noise factors and the assumptions made in the model. The measured values show a peak extinction of 2×10^3 (33 dB) at 1698 nm while the model predicts a peak extinction of 4.3×10^3 (36 dB) at 1678 nm. The extinction

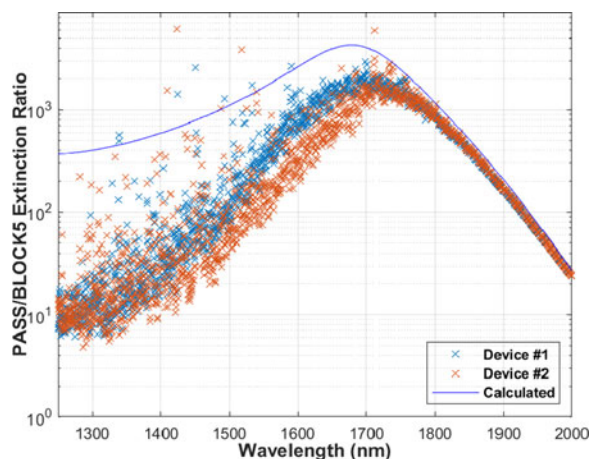


Fig. 7. Measured and calculated extinction ratio between the PASS state and the BLOCK5 state.

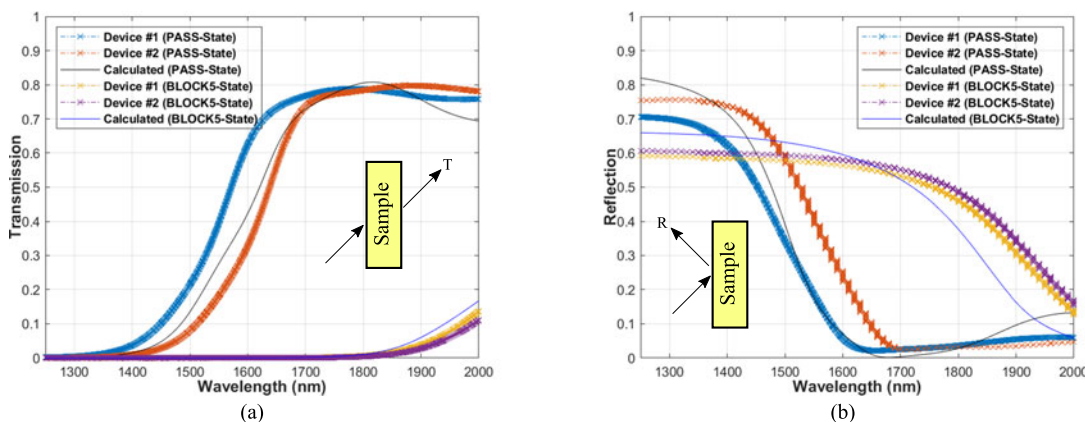


Fig. 8. Measured transmission and reflection (at 45-deg incidence) compared to the calculated results for the PASS and BLOCK5 states.

values are above 30 dB between 1500 nm and 1800 nm, which is a large spectral range of 300 nm. We believe this is the highest extinction ever reported in an optical limiting device over such a broad spectral range.

Fig. 8(a) and (b) show the measurement results obtained at a 45-deg incidence. The blue shift in the band edge can be seen, as expected, but the overall PASS and BLOCK performance remains largely unchanged. The calculated results were obtained by taking a linear average of the TE and TM values. The agreement with the model is slightly worse here, especially for the reflection, which is most likely because the films were characterized under normal incidence. But, the general shape and trend of the spectral curves is still consistent between the measured and calculated values.

5. Discussion

The results shown in this paper demonstrate that a multilayer thin film device using GST in an edge-filter configuration has the potential to be used as an optical limiter. Nevertheless, before conclusive claims can be made of its usefulness, it is important to discuss several aspects of this concept that require further investigation and development. The first consideration is the optical damage threshold. If the input pulse duration is longer than a nanosecond (this is the case in all practically important situations), the laser-induced damage to the limiter is predominantly heat-related. Moreover, in absorption-based optical limiters, the damage threshold is usually not much

higher than the limiting threshold, which makes such limiters ‘single-use’. They sustain irreversible damage after they switch to the BLOCK state. In contrast, the device demonstrated in this paper has a highly reflective BLOCK state. High reflectivity prevents overheating and thus dramatically increases the limiter survivability. Nevertheless, we should note that GST films are generally soft and easily scratched, therefore, their durability under intense laser illumination has to be verified. This could be particularly important because the imaginary part of the refractive index, κ , in the crystalline states is significantly higher than in the amorphous state. The second consideration is, although the intrinsic switching speed of GST from amorphous to crystalline phase has been shown to be in the picosecond to nanosecond scale, the overall switching of the device will occur layer-by-layer in a sequence that will be dictated by the optical field distribution. The thermal time constant of the system will also affect the switching sequence of the films, and will be an important consideration under pulsed laser illumination. Third, the ability to reset the films back to their PASS state is an important requirement. We have not addressed the resettability of the optical limiter in this work. Although this is routinely done in PCRAM devices, in the case of an optical limiter an additional laser beam may be necessary to induce the fast melt-quench process to amorphize the films. It may also be possible to utilize short electrical pulses via transparent metal electrodes or a wire grid to amorphize the films. Although the design presented in this work meets most of the objectives such as spectral bandwidth and extinction ratio, these additional factors will ultimately determine its viability in real applications.

6. Conclusions

We have experimentally demonstrated a reflective-style optical limiter/switch using repeating layers of $\text{Ge}_2\text{Sb}_2\text{Te}_5$ and SiO_2 in a photonic bandgap edge-filter configuration. Switching between the PASS and the BLOCK states occurs when the temperature of the GST layers rises above 145°C . The beneficial characteristics of this device are the broad spectral band and the wide acceptance angles of the PASS state, as well as the enhanced, broadband, and omnidirectional reflectance in the BLOCK states. When the GST layers switch from amorphous to cubic crystalline phase, the band edge shifts to a longer wavelength, producing a useful switching range of greater than 300 nm. Measured values show a maximum transmission greater than 80% and a peak extinction of 36 dB. Other aspects, such as resetting the device from BLOCK to the PASS state, damage thresholds, and transition dynamics have not been examined in this work.

References

- [1] E. W. Van Stryland, Y. Y. Wu, D. J. Hagan, M. J. Soileau, and K. Mansour, “Optical limiting with semiconductors,” *J. Opt. Society of Amer. B*, vol. 5, no. 9, pp. 1980–1988, Sep. 1988.
- [2] R. C. Hollins, “Materials for optical limiters,” *Current Opinion Solid State Mater. Sci.*, vol. 4, no. 2, pp. 189–196, Apr. 1999.
- [3] X. Sun, R. Q. Yu, G. Q. Xu, T. S. a. Hor, and W. Ji, “Broadband optical limiting with multiwalled carbon nanotubes,” *Appl. Phys. Lett.*, vol. 73, no. 25, pp. 3632–3634, Dec. 1998.
- [4] J. H. Vella *et al.*, “Experimental Realization of a Reflective Optical Limiter,” *Phys. Rev. Appl.*, vol. 5, no. 6, Jun. 2016, Art. no. 064010.
- [5] W. Wang, Y. Luo, D. Zhang, and F. Luo, “Dynamic optical limiting experiments on vanadium dioxide and vanadium pentoxide thin films irradiated by a laser beam,” *Appl. Opt.*, vol. 45, no. 14, pp. 3378–3381, May 2006.
- [6] O. B. Danilov *et al.*, “Optical limitation of Mid-IR radiation in vanadium dioxide films,” *Tech. Phys.*, vol. 48, no. 1, pp. 73–79, 2003.
- [7] S. Raoux and M. Wuttig, *Phase Change Materials*, S. Raoux and M. Wuttig, Eds. Boston, MA: Springer US, 2009.
- [8] J. Siegel, A. Schropp, J. Solis, C. N. Afonso, and M. Wuttig, “Rewritable phase-change optical recording in $\text{Ge}_2\text{Sb}_2\text{Te}_5$ films induced by picosecond laser pulses,” *Appl. Phys. Lett.*, vol. 84, no. 13, pp. 2250–2252, Mar. 2004.
- [9] M. Wuttig, H. Bhaskaran, and T. Taubner, “Phase-change materials for non-volatile photonic applications,” *Nature Photon.*, vol. 11, no. 8, pp. 465–476, Aug. 2017.
- [10] W. H. P. Pernice and H. Bhaskaran, “Photonic non-volatile memories using phase change materials,” *Appl. Phys. Lett.*, vol. 101, no. 17, Oct. 2012, Art. no. 171101.
- [11] A. Tittl *et al.*, “A switchable mid-infrared plasmonic perfect absorber with multispectral thermal imaging capability,” *Adv. Mater.*, vol. 27, no. 31, pp. 4597–4603, Aug. 2015.

- [12] R. E. Simpson *et al.*, "Toward the ultimate limit of phase change in $\text{Ge}_2\text{Sb}_2\text{Te}_5$," *Nano Lett.*, vol. 10, no. 2, pp. 414–419, Feb. 2010.
- [13] A. V. Kolobov, P. Fons, A. I. Frenkel, A. L. Ankudinov, J. Tominaga, and T. Uruga, "Understanding the phase-change mechanism of rewritable optical media," *Nature Mater.*, vol. 3, no. 10, pp. 703–708, Oct. 2004.
- [14] N. Yamada, "Origin, secret, and application of the ideal phase-change material GeSbTe ," *Physica Status Solidi (b)*, vol. 249, no. 10, pp. 1837–1842, Oct. 2012.
- [15] B.-S. Lee, J. R. Abelson, S. G. Bishop, D.-H. Kang, B.-k. Cheong, and K.-B. Kim, "Investigation of the optical and electronic properties of $\text{Ge}_2\text{Sb}_2\text{Te}_5$ phase change material in its amorphous, cubic, and hexagonal phases," *J. Appl. Phys.*, vol. 97, no. 9, May 2005, Art. no. 093509.
- [16] T. Ouled-Khachroum *et al.*, "Stress buildup during crystallization of thin chalcogenide films for memory applications: In situ combination of synchrotron X-Ray diffraction and wafer curvature measurements," *Thin Solid Films*, vol. 617, pp. 44–47, 2016.
- [17] T. Matsunaga, N. Yamada, and Y. Kubota, "Structures of stable and metastable $\text{Ge}_2\text{Sb}_2\text{Te}_5$, an intermetallic compound in $\text{GeTeSb}_2\text{Te}_3$ pseudobinary systems," *Acta Crystallographica Section B Structural Sci.*, vol. 60, no. 6, pp. 685–691, Dec. 2004.
- [18] E. M. Vinod, K. Ramesh, R. Ganesan, and K. S. Sangunni, "Direct hexagonal transition of amorphous $(\text{Ge}_2\text{Sb}_2\text{Te}_5)_{0.9}\text{Se}_{0.1}$ thin films," *Appl. Phys. Lett.*, vol. 104, no. 6, Feb. 2014, Art. no. 063505.
- [19] A. Macleod, *Thin-Film Optical Filters*, 4th ed. New York, NY, USA: Taylor & Francis, 2010.